Proceedings of the 3rd International Conference on Mathematical Physics and Computational Simulation
DOI: 10.54254/2753-8818/100/2025.21443

Discovery of a Partially Obscured Supermassive Binary Black Hole System

Youyi Sun[1,a,*]

[1]*Shanghai Pinghe School, Shanghai, China*
a. 18994981660@163.com
**corresponding author*

Abstract: Galaxy mergers are a crucial pathway for the growth and evolution of galaxies at the cosmic center. Supermassive black holes (SMBHs) are commonly present at the centers of galaxies. During galaxy mergers, the central SMBHs may form binary black hole systems and, in some cases, merge. Detecting and studying supermassive binary black hole systems within galaxies is a significant aspect of galaxy evolution research. Active black holes produce prominent broad emission lines, which serve as effective probes of such activity. The presence of two distinct sets of broad emission lines with velocity differences has traditionally been considered a key indicator for identifying binary black holes. However, the probability of both black holes in a binary system being active is extremely low. More commonly, binary systems consist of one active and one quiescent black hole. The spectral signature of such systems is characterized by a significant velocity offset $\Delta v > 1000$ km/s between the broad emission lines and the system's narrow emission lines. This velocity difference has also led to the discovery of "recoiling" black holes, driven by gravitational wave radiation from closely bound binary systems. Recoiling black holes are crucial observational targets for studying black hole mergers, binary orbital evolution, and galaxy mergers.We have identified a class of recoiling black holes with partially obscured nuclear regions. Dust in the nuclear region attenuates the intense radiation from the active black hole, allowing the host galaxy's emission to become visible alongside the nuclear radiation and broad-line features. This discovery provides a unique perspective for exploring the physical connection between the evolution of binary black hole systems and galaxy evolution. Further studies using multi-wavelength photometry, high-resolution spectroscopic analysis, and long-term spectral monitoring of partially obscured supermassive binary black hole systems are expected to reveal the physical processes underlying black hole mergers and galaxy mergers, as well as their significant role in galaxy evolution.

Keywords: galaxy mergers, binary black hole systems, supermassive black holes, active galactic nuclei

1. Introduction

1.1. Supermassive Black Hole in Milky Way

The 2020 Nobel Prize in Physics was awarded to three laureates for their discoveries related to one of the most enigmatic phenomena in the universe—black holes. Black holes capture everything that

DOI: 10.54254/2753-8818/100/2025.21443

enters their vicinity, including light. Roger Penrose demonstrated that black holes are a direct consequence of general relativity, employing ingenious mathematical methods. Reinhard Genzel and Andrea Ghez discovered the SMBH at the center of our Milky Way. Their decades-long precise observations of stars near the galactic center revealed the presence of an invisible, immensely massive object, whose gravitational influence governs the closed orbits of the surrounding stars.

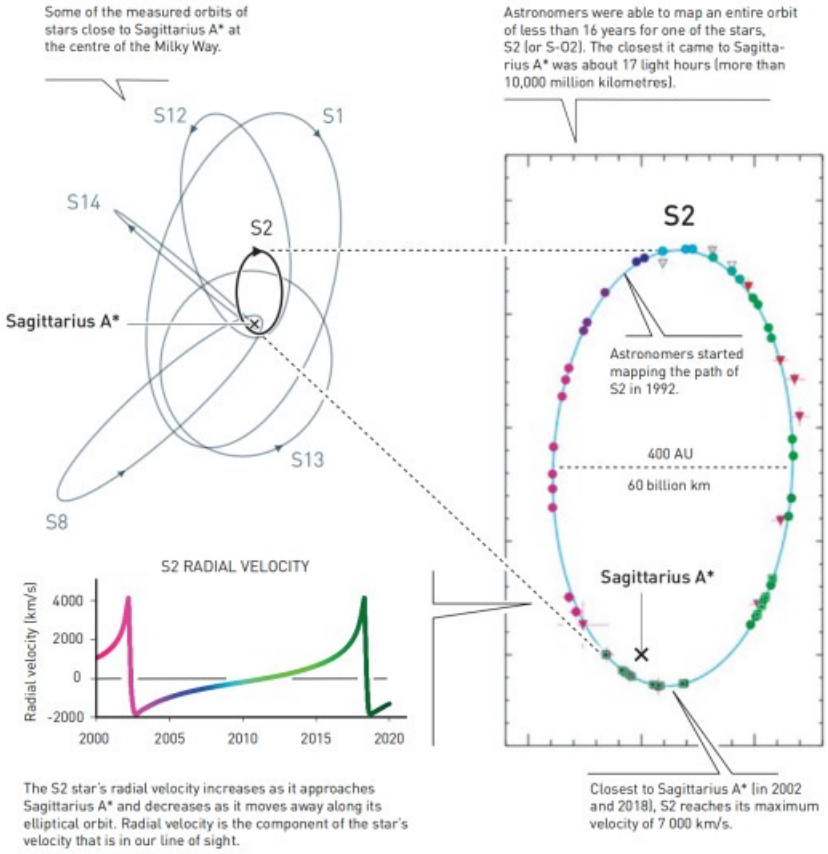

Figure 1: The orbital paths of stars S2, S12, S14, S13, and S8 are utilized to map the spatial structure surrounding the SMBH at the Galactic Center. The figure highlights the radial velocity variations of the star S2 over time. As S2 approaches Sagittarius A* along its elliptical trajectory, its radial velocity increases, reaching a peak of 7000 km/s during its closest approaches in 2002 and 2018. Conversely, as the star moves away from Sagittarius A*, its radial velocity decreases. Radial velocity, defined as the component of a star's velocity along the observer's line of sight, is a critical parameter for understanding the gravitational influence of the SMBH and the kinematics of nearby stellar objects .

The smallest orbit, that of the star S2, spans approximately 40 astronomical units (AU), comparable to the size of the solar system, with an orbital period of about 20 years. According to Keplerian orbital mechanics, the central object's mass is estimated to be around 4 million solar masses. For such a massive object confined to such a small space, the only plausible explanation is a SMBH.

However, observations are extremely challenging, as the Galactic Center is 8 kiloparsecs (kpc) from Earth and is heavily obscured by dense dust clouds in the optical spectrum. Genzel and Ghez employed advanced adaptive optics and infrared imaging technology to track the orbits of approximately 30 stars with unprecedented precision. Recently, the SMBH at the center of the Milky Way was directly imaged by the Event Horizon Telescope.

The discovery of an SMBH in the Milky Way has profound implications for astrophysics. It confirms the existence of these cosmic giants and provides a unique laboratory for testing

DOI: 10.54254/2753-8818/100/2025.21443

gravitational theories and studying accretion processes near the event horizon. Recent observations and research indicate that SMBHs exist in nearly all galaxies, situating the Milky Way within a broader cosmic framework. SMBHs are now understood to be indispensable to both galaxy evolution and their own growth.

1.2. Supermassive Black Holes in Galaxies

In modern astrophysics, the paradigm that every massive galaxy hosts a SMBH at its core has become increasingly well-established, supported by extensive observational evidence across various wavelengths and techniques. The foundational work of Ferrarese et al. [1] demonstrated a strong correlation between the mass of central SMBHs and the stellar velocity dispersion of their host galaxies, expressed as $M_{bh} \propto \sigma_c^{4.8\pm0.5}$. This relationship allows the mass of SMBHs to be estimated using simple, low-resolution measurements of stellar velocity dispersion, providing crucial insights into the coevolution of black holes and their host galaxies.

1.3. Supermassive Black Holes in Active Galactic Nuclei

The masses of SMBHs range from millions to billions of solar masses, and they are central to the phenomenon of AGN. The presence of SMBHs is inferred from the broad emission lines observed in AGN spectra, which indicate gas moving at high velocities near a massive object. Using the virial theorem, astronomers estimate the masses of these black holes based on the observed velocities and the widths of the emission lines.

AGN energy output is often described as a "featureless continuum," resulting from the accretion of matter onto SMBHs. This process converts gravitational potential energy into radiation, illuminating the surrounding environment and producing the multi-wavelength emissions observed in AGN.

A key aspect of studying SMBHs in AGN is understanding their coevolution with their host galaxies. Empirical correlations, such as the M-sigma relationship, link the mass of SMBHs to the velocity dispersion of their host galaxies' bulges, highlighting a profound connection between SMBH growth and galaxy evolution.

SMBHs in AGN remain a critical area of astrophysics, offering insights into galaxy formation, black hole dynamics, and cosmic feedback processes. With advancing observational technologies, our understanding of these cosmic giants and their role in the universe will continue to deepen.

1.4. Binary Black Holes in Active Galactic Nuclei

The study of binary SMBHs in active galaxies has opened new avenues for understanding galaxy evolution and SMBH dynamics. The pioneering work of Eracleous & Halpern [2] in “The Astrophysics of Binary Black Holes” provides a comprehensive analysis of the observational characteristics and theoretical implications of binary SMBHs, with a particular focus on the optical spectroscopic features that reveal their presence.

The optical spectra of active galaxies hosting binary SMBHs often exhibit complex patterns, such as double-peaked emission lines, indicative of distinct accretion processes around each black hole. These spectral features, detailed extensively by Eracleous [2], are critical for identifying and studying binary SMBH systems. The paper highlights the transient nature of the binary stage on cosmological timescales and emphasizes the importance of high-resolution spectroscopy for capturing the subtle spectral features of these systems.

Current research delves into the dynamics of these systems, exploring how gravitational interactions between the two SMBHs affect orbital decay and eventual merger. Studying these binary

DOI: 10.54254/2753-8818/100/2025.21443

systems is crucial for understanding the role of SMBH mergers in the generation of gravitational waves, an emerging field in observational astronomy[3] .

One major conclusion of these studies is that binary SMBHs are not only natural outcomes of galaxy mergers but also play key roles in feedback mechanisms regulating star formation and the growth of their host galaxies. Interactions between SMBHs can trigger gas ejections within galaxies, influencing their evolutionary pathways.

Fundamentally, binary SMBHs in active galaxies exemplify the intricate interplay between cosmic structures and processes. As observational technologies continue to advance, we can expect to uncover more about these enigmatic systems, their formation mechanisms, and their impact on the broader universe.

2. Theories

SMBHs are located at the centers of many galaxies. In the cores of these galaxies, the gravitational pull of the black hole attracts surrounding gas, forming complex structures, with the most prominent being the accretion disk, broad-line region (BLR), and narrow-line region (NLR) (as shown in Figure 2.1). These regions are crucial not only for understanding the physical state of the black hole but also for providing important clues about the interactions between the black hole and its host galaxy. Specifically, in binary black hole systems, the spectral characteristics of these regions may exhibit unique variations, providing key information for detecting and studying such systems.

In AGN, SMBHs are often accompanied by an accretion disk, a rotating structure of gas orbiting the black hole. Within the accretion disk, due to frictional forces, the gas gradually spirals inward and moves toward the black hole's center, eventually being accreted. This process is one of the main ways in which the black hole grows. As the gas accelerates inward, gravitational potential energy is converted into thermal energy, heating the gas and emitting intense radiation, which forms the continuous spectrum observed.

The region close to the accretion disk is known as the broad-line region (BLR). In this region, the gas, due to its proximity to the black hole, moves at extremely high speeds, reaching up to 5000 km/s in Keplerian motion. This high velocity results in significant Doppler broadening of the emitted spectral lines, forming the broad emission lines observed. These broad emission lines are one of the key features of AGN spectra, indicating the presence of high-velocity gas around the black hole. Therefore, in binary black hole systems, the spectral features of the BLR may change due to interactions between the two black holes. If the two black holes are close enough, their BLRs may merge into a single broad-line region, or remain separate, forming a double-peaked structure. This double-peaked structure appears in the spectrum as two peaks in the broad emission lines, a significant characteristic of binary black hole systems.

In contrast, the narrow-line region (NLR) is located farther from the black hole, where the gas moves at slower speeds, approximately 500 km/s, and typically exhibits a conical distribution. Due to the slower motion, the spectral lines emitted by the gas in the NLR are narrower. These narrow emission lines also play a crucial role in the spectral analysis of AGN. They are often used to study other physical processes in the galactic nucleus, such as star formation.

DOI: 10.54254/2753-8818/100/2025.21443

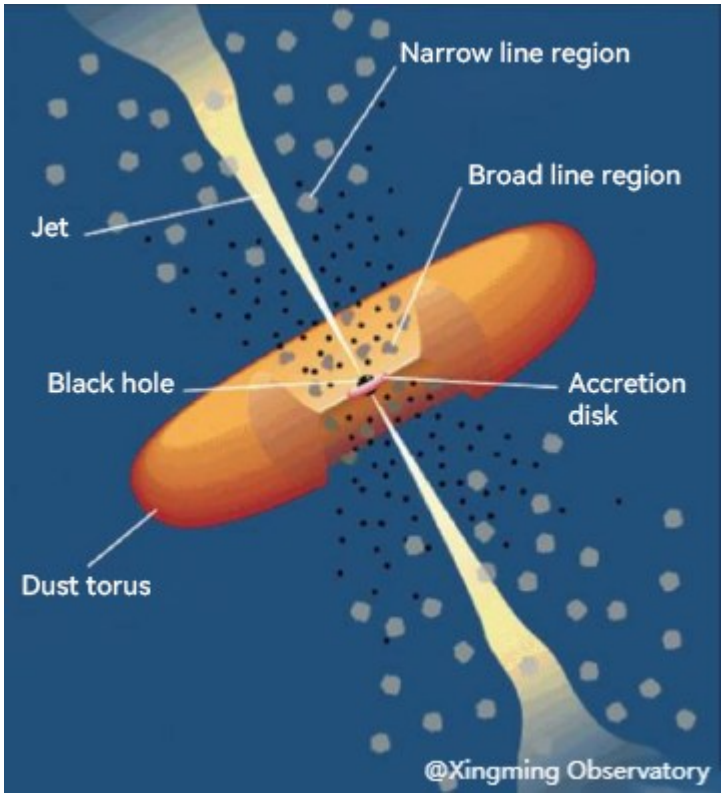

Figure 2: The structure of gas around the black hole, including the black hole, accretion disk, broad-line region, torus, narrow-line region, and jet-emitting areas.

2.1. Cosmological Redshift and Doppler Redshift

The concept of redshift is crucial for understanding the cosmological implications of AGN. In "Astrophysics in a Nutshell" (p. 209), the author discusses the experimental predictions of cosmological models, including cosmological redshift, which is a direct result of the expansion of the universe. Redshift is mathematically described by the null geodesic equation for photons propagating through the Friedman-Robertson-Walker (FRW) metric:

$$0 = c^2 \frac{dt^2}{R(x)^2} - \frac{1}{1-kr^2} \frac{dr^2}{R(t)^2} \tag{1}$$

This equation illustrates the fundamental principles behind Hubble's Law, which connects the redshift of galaxies with their distance from us, indicating the expansion of the universe[4].

In "An Introduction to Active Galactic Nuclei" (p. 78), the author delves into the Doppler redshift observed in AGN, particularly in the context of the broad-line region (BLR). Evidence suggests the presence of an optically thin component within the BLR that affects the observed spectral lines. For instance, in Seyfert galaxies, differences in line profiles between optically thick and thin clouds have been observed, indicating the diversity in the properties of clouds within the BLR [5].

2.2. Structure of Active Galactic Nuclei

An AGN refers to a galaxy with a SMBH at its center. The black hole at the galaxy's core releases immense energy by accreting surrounding matter, including gas, dust, and celestial objects, making AGNs some of the brightest objects in the universe.

DOI: 10.54254/2753-8818/100/2025.21443

At the center of an AGN is a SMBH, with masses ranging from around one million solar masses to over ten billion solar masses. The accretion activity of the black hole is the primary energy source responsible for the luminosity of the AGN.

The region around the black hole is composed of gas and dust and is referred to as the accretion disk. In this region, matter gradually moves toward the center of the black hole and is heated to extremely high temperatures, emitting intense electromagnetic radiation, spanning from radio waves to X-rays and gamma rays. This region is also a significant source of the continuous spectrum.

Outside the accretion disk lies a region composed of high-temperature gas surrounding the black hole, known as the broad emission line region (BLR). The gas in this region is excited by the intense radiation emitted by the central black hole. The broadening of the emission lines is primarily due to the high-speed motion of the gas, including its rotation, turbulence, and radial motion. The central wavelengths of these lines are related to the types of elements in the gas and their ionization state, while the motion of the gas determines the width and shape of the emission lines.

Further out from the BLR is the narrow emission line region (NLR), where narrow emission lines are detected in the spectrum. The broadening of these narrow emission lines is mainly due to the slower movement of the gas, such as expansion and outflows. The central wavelengths of these lines are also determined by the gas's elemental composition and ionization state. The narrower width of the emission lines, compared to those in the BLR, reflects the lower velocity of the gas.

2.3. Spectra of Active Galactic Nuclei

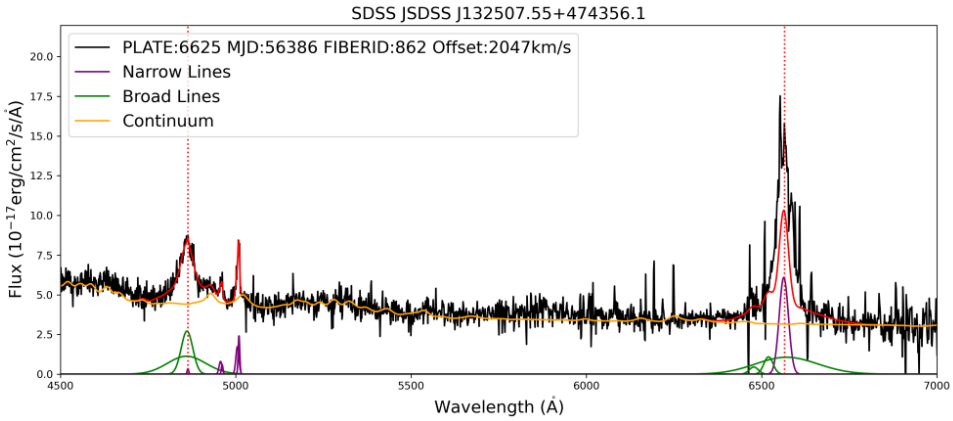

Figure 3: The spectrum of the AGN SDSS J132507.55+474356.1. It includes the broad lines (green), narrow lines (purple), and the continuum (yellow). The wavelength range spans from 4500 Å to 7000 Å, with flux in units of (10^-17 erg/cm^2/s/A). The Hβ and Hα emission lines are marked with red dashed lines at wavelengths of 4862.68 Å and 6564.61 Å, respectively.

In this study, we gained further insight into the structure of AGN by analyzing a spectrum of an actual active galaxy. As shown in the figure, the yellow line represents the continuum, originating from the thermal radiation of the accretion disk. The green line represents the broad emission lines, and the purple line represents the narrow emission lines. On the left side of the spectrum, we observe a prominent broad emission line, the Hβ line, while on the right side, we find the Hα line. Through careful measurement of these two emission lines, we found their broadening to be approximately 5000 km/s, which aligns with the high-velocity motion of gas in the broad-line region. Additionally, it is clear from the spectrum that the broadening of the narrow emission lines is significantly smaller than that of the broad emission lines, indicating that the gas in the narrow-line region moves more slowly than that in the broad-line region. This difference reflects the different dynamical states of the

DOI: 10.54254/2753-8818/100/2025.21443

gas in the two regions, with the gas in the broad-line region being strongly influenced by the black hole's gravity, while the gas in the narrow-line region is relatively more quiescent.

In the spectral analysis of AGN, the width of the emission lines provides an effective method for measuring the mass of the central SMBH. The broad emission lines in AGNs are primarily generated by the broad-line region surrounding the black hole. The gas in these regions moves at velocities close to Keplerian speeds. Therefore, by measuring the Doppler width of these broad emission lines and using the Doppler formula $c \times \frac{\Delta\lambda}{\lambda_0}$, we can estimate the orbital velocity of the gas. From the orbital velocity of the gas, we can further estimate the mass of the central black hole:

$$M_{BH} \propto \frac{v^2}{GM_{encl}} \left(\frac{r}{GM_{BH}/c^2}\right)^{1/2} \tag{2}$$

2.4. Spectral Characteristics of Binary Black Holes

In the spectrum of binary black holes, two distinct sets of broad emission lines can be observed. This is because each set of broad emission lines originates from the active region of each SMBH. They reveal the relative motion of the gas near the black holes, where the gas is accelerated by the gravitational pull of the black holes and emits radiation. These broad emission lines show two separated peaks, which result from the Doppler redshift and blueshift effects caused by the relative motion of the two black holes.

However, such a double-peaked structure is not present in the spectra of ordinary galaxies (which contain only one SMBH at their center), as shown in the spectra of normal galaxies and active galaxies in Figures 2.41 and 2.42. It is precisely because the spectrum of a binary black hole system has such features that it provides a more intuitive way to detect binary black hole candidates.

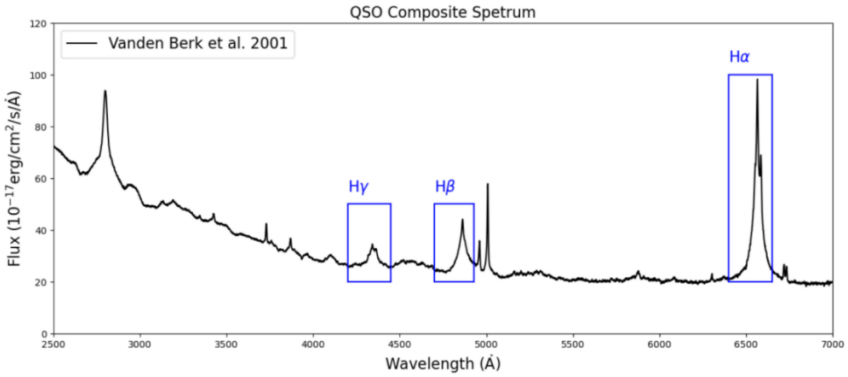

Figure 4: Spectrum of a Typical AGN

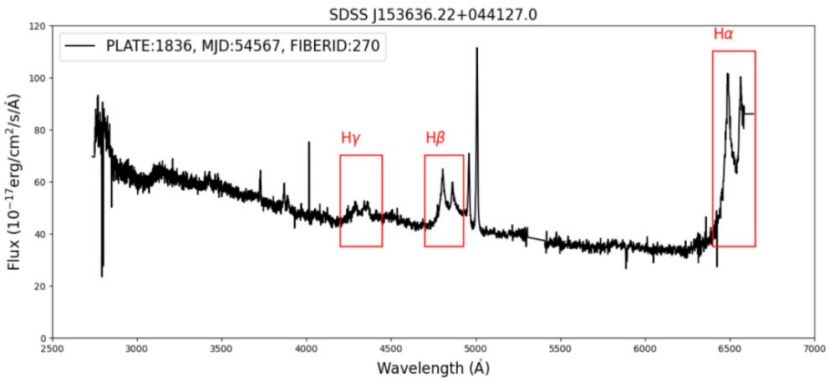

Figure 5: Spectrum of a Typical AGN with Binary Black Holes

DOI: 10.54254/2753-8818/100/2025.21443

Comparing Figures 2.41 and 2.42, it is evident that the broad emission lines in the spectra of binary AGN and typical AGN are markedly different. From the upper figure, it is clear that the broad emission lines in binary AGN each exhibit two peaks, corresponding to the AGN driven by the respective black holes.

However, because active black holes constitute a very small proportion of galaxies, and the proportion of both black holes being active in two galaxies is even lower, we often observe binary black hole systems composed of one active black hole and one inactive black hole. In such cases, it is very difficult to observe spectra with double-peaked structures. Therefore, our study primarily focuses on the characteristic of significant velocity differences between the broad and narrow lines in the spectra of binary black holes.

In addition to the double-peaked structure feature, the wavelengths of the narrow and broad lines in the spectra of binary black hole systems also exhibit significant velocity differences. This is because the broad lines are signals that describe the motion of the black holes, while the narrow lines are signals that describe the entire galaxy. In the case of two black holes orbiting each other, their motions are very intense, much more so than the motion of black holes in typical galactic centers, but the galaxy's motion relative to the black holes is not intense. Therefore, the broad and narrow lines form a significant velocity difference, which also becomes an important factor in determining the spectra of binary black holes.

Figure 2.5 illustrates a binary black hole system composed of an active black hole and an inactive black hole. In these two black holes, one black hole has an accretion rate significantly higher than the other and carries the only broad emission line region in the system, making the system resemble a single-line spectroscopic binary. Consequently, our primary research focus is on identifying spectra where there is a significant velocity difference between the broad lines and the narrow lines. Such cases are further categorized into orbital motion and recoil phenomena.

2.5. Spectral Characteristics of Binary Black Holes — Spectral Features of "Recoiling" Black Holes

In the study by Komossa, Zhou, and Lu (2008), they proposed a strong candidate for a recoiling SMBH—located in the quasar SDSS J092712.65+294344.0. This also provides observational characteristics of another black hole and its host galaxy for this research.

In binary black hole systems, when two black holes ultimately merge through gravitational wave radiation, the system generates a recoil force according to the conservation of momentum. This causes the merged black hole to acquire a certain velocity, potentially ejecting it from the center of its host galaxy. The magnitude of this recoil effect depends on several factors, including the spin directions of the black holes, the mass ratio, and their relative orbital parameters before the merger.

However, not all binary black hole mergers result in noticeable recoil phenomena. The existence of a recoiling black hole depends on specific conditions, such as whether the two black holes have sufficient spin and whether their spins are aligned with their orbital angular momentum. If the spin directions of the two black holes are opposite (anti-parallel) to their orbital angular momentum, the gravitational waves emitted during their merger will have an asymmetric radiation pattern, resulting in a greater recoil velocity. According to numerical simulations, such recoil velocities can reach several thousand kilometers per second.

The quasar SDSS J092712.65+294344.0 exhibits two sets of distinct emission lines: one set consists of very narrow emission lines, and the other set comprises broad Balmer lines and broad high-ionization forbidden lines. These broad emission lines are blue-shifted relative to the narrow emission lines by approximately 2650 kilometers per second. The most natural explanation for these observations is that the SMBH has been ejected from the galaxy's core during the merger, simultaneously carrying away the broad-line gas while leaving behind most of the narrow-line gas.

DOI: 10.54254/2753-8818/100/2025.21443

This indicates that the gravitational waves produced by the black hole merger not only caused the recoil of the black hole itself but also affected the surrounding gas.

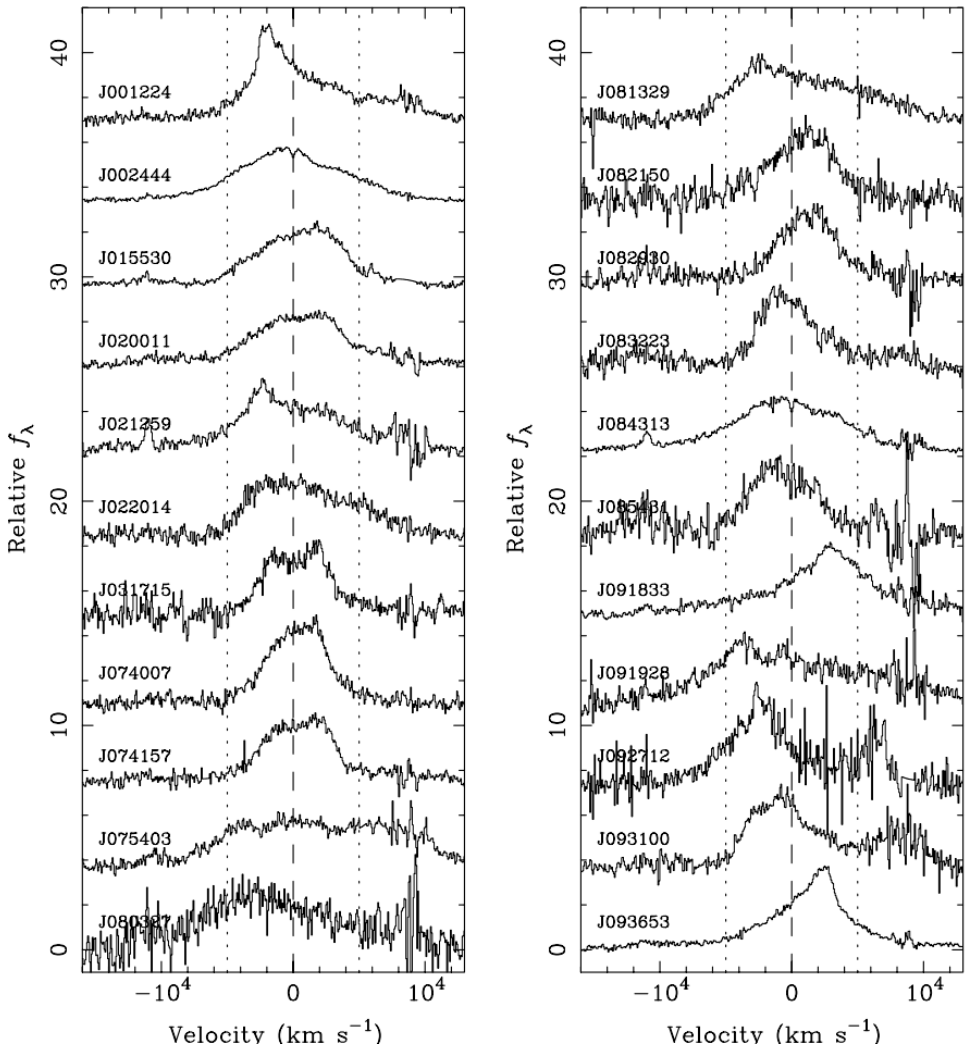

Figure 6: The profile of the broad Hβ line in the SDSS spectrum on a common velocity scale. The narrow Hβ line, O[III] line, and underlying continuum have been subtracted. The resulting profile has been arbitrarily normalized and vertically offset from each other for clarity. The vertical dashed lines indicate the positions of the narrow Hβ line, while the vertical dotted lines mark a window of ±5000 km/s from that line. The noise frequently observed at +8875 km/s is caused by the imperfect subtraction of the O[III] λ5007 line. The subtracted He[II] λ4686 line can sometimes be identified at -10800 km/s.

Therefore, although not all binary black hole systems necessarily produce recoiling black holes, under specific conditions—such as when the black holes possess sufficient spin and their spin directions are opposite to their orbital angular momentum—the merger of binary black holes can indeed generate sufficiently large recoil velocities to completely eject the SMBH from the center of its host galaxy. The detection of such recoiling black holes is of significant importance for understanding the formation and evolution of black holes and galaxies, the generation of gravitational waves, and the growth patterns of black holes during the early periods of cosmic structure formation[6].

DOI: 10.54254/2753-8818/100/2025.21443

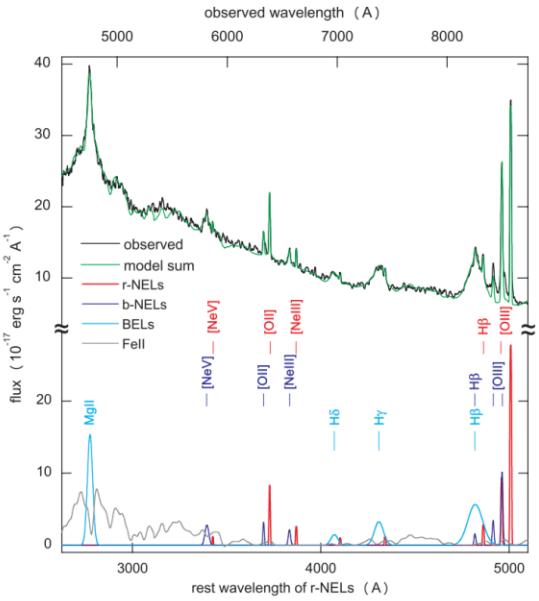

Figure 7: The SDSS spectrum of SDSS J0927+2943 displays two sets of emission lines separated by a velocity redshift of approximately 2650 km/s. Red: one set of narrow emission lines (r-NELs). Blue and light blue: another set of emission lines (b-NELs and BELs, respectively). Gray: Fe[II] spectrum.

2.6. Spectra of Galaxies

After establishing the sample, we will analyze the spectra of the target galaxies (including physical properties and spectral characteristics). The website used is Firefly (http://www.icg.port.ac.uk/firefly/).

Firefly is a chi-square minimization fitting code used to derive the stellar population properties of stellar systems, whether from observed galaxy or cluster spectra or from simulated model spectra. Firefly fits combinations of single stellar population (SSP) models to the spectral data, following an iterative best-fit process controlled by the Bayesian Information Criterion. No prior assumptions are applied; instead, all solutions within the statistical cutoff range and their weights are retained arbitrarily. Additionally, no additive or multiplicative polynomials are used to adjust the spectral shape, nor is any regularization imposed. This fitting freedom allows the depiction of how intrinsic spectral energy distribution (SED) degeneracies (such as age, metallicity, and dust extinction) affect stellar population properties and quantifies the impact of different input model components on these properties. Dust extinction is included using a new program that employs a Gaussian filter (HPF) to perform fitting after correcting the continuum. The resulting extinction array is then matched with known analytical approximations to return the E(B-V) values. This process removes large-scale spectral patterns related to dust and/or poor flux calibration. The fitting method has been extensively tested through simulated galaxies, real galaxies from the Sloan Digital Sky Survey, and globular clusters in the Milky Way. The robustness of the derived properties has been evaluated as a function of signal-to-noise ratio and the adopted wavelength range. Firefly is capable of reliably recovering age, metallicity, stellar mass, and even star formation history in systems with a signal-to-noise ratio of approximately 5, making it suitable for moderately dusty systems.

Firefly provides the best-fit model and its components' light weights and mass-weighted stellar population properties—age, metallicity, E(B-V), stellar mass, and their distribution in remnants (white dwarfs, neutron stars, black holes). It provides the star formation rates for each component, and the overall past average can be easily derived from the provided quantities. By plotting the

DOI: 10.54254/2753-8818/100/2025.21443

weighted SSP contributions, the star formation history can be easily inferred. The errors in these properties are obtained through the likelihood of solutions within the statistical cutoff range.

The code, in principle, can fit any model to any spectrum, any spectral resolution, and any wavelength range. Currently, the code has been applied to spectra from SDSS, integral field units (MANGA), the DEEP2 survey, and globular clusters from various sources.

A complete description of the code and the results of extensive testing can be found in Wilkinson et al. (2017). Updates for version 1.0.1, further performance tests, and comparisons between different settings can be found in Neumann et al. (2022).。

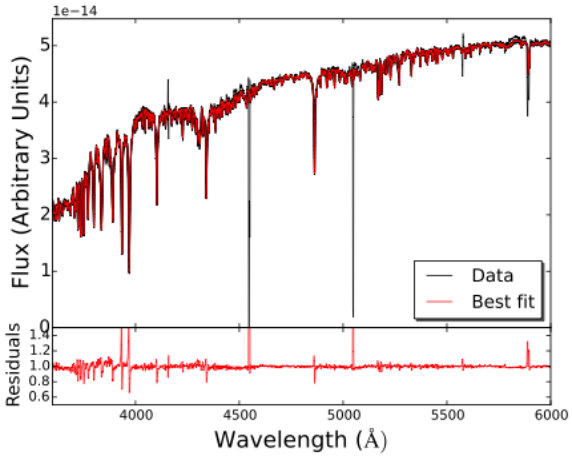

Figure 8: The observed data (Data), the best-fit stellar population model (Best fit), and the residuals between the two (Residuals). The wavelength axis ranges from 4000 Å to 6000 Å, covering the key spectral range used to determine the stellar population properties of the galaxy. The close correspondence between the data and the best-fit model indicates a good fit, while the residuals plot reveals the differences between the model predictions and the actual observations. [7]

3. Data Analysis

3.1. Properties of Quasars from SDSS DR16

The study by Qiaoya Wu and Yue Shen [8] provides a spectral catalog of 750,414 broad-line AGN spectra, all sourced from the Sloan Digital Sky Survey Data Release 16 AGN catalog (DR16Q). The redshift range of these AGNs spans from 0.1 to 6, and their luminosity range covers $44 \leq \log(L_{bol}/\text{erg s}^{-1}) \leq 48$. The final catalog includes a continuum and spectral characteristics of a series of prominent emission lines in quasar spectra, as well as derived quantities such as black hole masses based on single-epoch mass prescriptions and Eddington ratios. This study represents a significant update to the 105,783 quasars cataloged in Shen et al. [8]from SDSS DR7. Compared to the DR7 catalog, DR16Q features a more comprehensive line list and an extension to lower-luminosity quasars. Additionally, DR16Q provides refined systemic redshifts and more accurate redshift uncertainties, showing substantial improvements over the original redshifts.

The research developed a Python program QSQFit for fitting quasar spectra. It offers a range of functions and methods to process and analyze quasar spectral data. For fitting the continuum, the program defines a residuals function within the _Fitter object, fitting a combination of power-law and cubic polynomial. The program employs the kmpfit. Fitter object to perform non-linear least squares fitting. For the Fe II emission lines in the UV and optical bands of the continuum, the code utilizes

DOI: 10.54254/2753-8818/100/2025.21443

the Fe_flux_magii and Fe_flux_balmer functions. For fitting emission lines, the program uses the _DoLineFit method to fit Gaussian functions to emission lines in specific line complexes (including Hα, Hβ, Mg II, C IV, etc.) in quasar spectra. It supports binding parameters such as the central wavelength, width, and flux of specific emission lines to enhance the stability and accuracy of the fits, and it provides local fitting capabilities for narrow emission lines. The results are then saved to FITS files, including continuum parameters and emission line parameters. The fitted parameters allow for the estimation of physical quantities such as black hole mass, luminosity, and Eddington ratio. These physical quantities are estimated in subsequent Fit methods, where parameters like LOGMBH_HB, LOGMBH_MGII, and LOGMBH_CIV are used to calculate black hole masses. Additionally, the program estimates the uncertainties of the fitted parameters through Monte Carlo simulations (using the _conti_mc and _line_mc methods), identifies and excludes outliers using Chauvenet's criterion, and detects anomalous points through variance analysis. For spectra with non-Gaussian characteristics, the program employs Gaussian-Hermite series for further fitting. Furthermore, the program offers the capability to fit two-dimensional data. This suite of programs is highly useful for assisting in the analysis and understanding of quasar spectral features, including both the continuum and emission lines, thereby facilitating a comprehensive analysis of quasar spectra[8].

This study is also immensely beneficial for our search for binary black holes. In binary black hole systems, the gravitational interactions between the two black holes lead to complex gas dynamics, resulting in double-peaked or broader emission lines. These can be reflected in the fitted parameters of emission lines by the program. Specifically, the full width at half maximum (FWHM) and peak wavelengths of the broad emission lines can help identify potential binary black hole systems. Moreover, by analyzing the width and shape of the emission lines in conjunction with redshift information, candidate binary black holes can be determined.

The program filters spectra based on redshift and signal-to-noise ratio (SNR) to ensure data quality and reliability. Spectra with too low SNR cannot provide reliable estimates of physical quantities and are excluded. Spectra with excessively high redshifts are unsuitable for our observational range and the capabilities of our instruments and are also excluded. In our study, redshifts are selected to be less than 0.52 to ensure that Hα is within the observable range. Our research focuses on Hα and Hβ because these are the two most prominent emission lines in quasar spectra. Additionally, spectra with an SNR greater than 5 are selected to ensure that the spectra are sufficiently clear. This selection process ensures that the chosen sample's spectral data can provide the most accurate physical quantity estimates, thereby enhancing the reliability of our statistical studies of AGN.

3.2. Determination of Broad Emission Line Velocity Offset

The velocity offset of the black hole can be represented by the peak wavelength of the broad Hα emission line, and the systemic velocity of the quasar can be represented by the peak wavelength of the narrow O[III] component. Therefore, the velocity difference (Δv) can be expressed as:

$$\Delta v = c\left(\frac{\lambda_{H\alpha}^{obs}-\lambda_{H\alpha}^{lab}}{\lambda_{H\alpha}^{lab}} - \frac{\lambda_{O[III]}^{obs}-\lambda_{O[III]}^{lab}}{\lambda_{O[III]}^{lab}}\right) \quad (3)$$

Where, Δv is the velocity difference; c is the speed of light, taken as 3×10^8 m/s; $\lambda_{H\alpha}^{obs}$ is the observed peak wavelength of the broad Hα emission line; $\lambda_{H\alpha}^{lab}$ is the laboratory peak wavelength of the broad Hα emission line; $\lambda_{O[III]}^{obs}$ is the observed peak wavelength of the narrow O[III] emission line; and $\lambda_{O[III]}^{lab}$ is the laboratory peak wavelength of the narrow O[III] emission line.

DOI: 10.54254/2753-8818/100/2025.21443

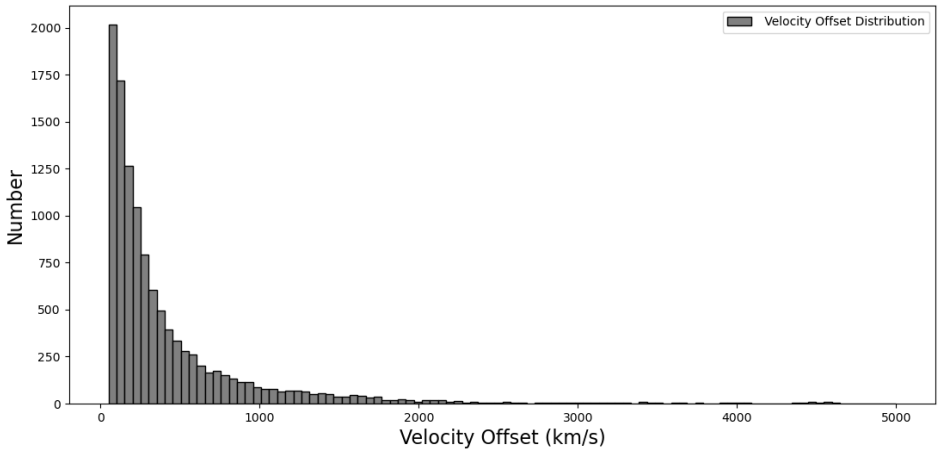

Figure 9: The statistical results of velocity offsets between broad and narrow emission lines in multiple quasars or AGN. The horizontal axis represents the velocity offset, measured in kilometers per second (km/s), ranging from 0 km/s to 5000 km/s. The vertical axis indicates the number of objects within each velocity offset interval, illustrating the frequency distribution of different velocity offset values.

3.3. Binary Black Hole Candidates

We obtained galaxy spectral data from the Sloan Digital Sky Survey (SDSS) and visualized the spectra individually using a Python program. After meticulous manual identification, we established 20 binary black hole candidates.

We constrain the velocity offsets of the samples to be between 1000 km/s and 4000 km/s, selecting targets with normal broad and narrow line profiles to avoid the impact of defective spectra in the following examples on our sample quality and judgments:

Table 1: All Selected Binary Black Hole Candidate Samples

	SDSS	PLATEID	MJD	FIBERID	Offset Velocity
1	J010950.37+335932.9	6594	56272	668	3315 km/s
2	J074920.00+234104.4	1204	52669	310	1084 km/s
3	J081032.72+565105.2	7280	56709	690	1238 km/s
4	J091525.27+463915.9	7314	56990	90	1469 km/s
5	J094603.94+013923.6	480	51989	480	1012 km/s
6	J111537.94+542725.3	8171	57135	156	2055 km/s
7	J112407.03+131651.3	5370	56003	356	1188 km/s
8	J113447.34+100736.4	1224	52765	400	3121 km/s
9	J114537.77+052225.0	839	52373	494	1663 km/s
10	J121522.77+414620.9	1450	53120	141	2469 km/s
11	J122006.84+065232.4	5397	55944	412	1192 km/s
12	J124529.19+134131.4	5410	56016	306	1385 km/s
13	J132704.13+443504.9	8378	57785	916	1498 km/s
14	J152402.19+255117.3	3960	55663	846	1471 km/s
15	J153636.22+044127.0	1836	54567	270	3402 km/s
16	J171448.50+332738.3	2973	54591	190	2529 km/s
17	J172553.34+383154.3	10762	58390	943	1652 km/s
18	J212843.41+002435.6	9180	57693	546	1914 km/s
19	J220246.31+012128.9	4316	55505	413	1366 km/s
20	J234623.42+010918.1	9178	58081	477	2251 km/s

DOI: 10.54254/2753-8818/100/2025.21443

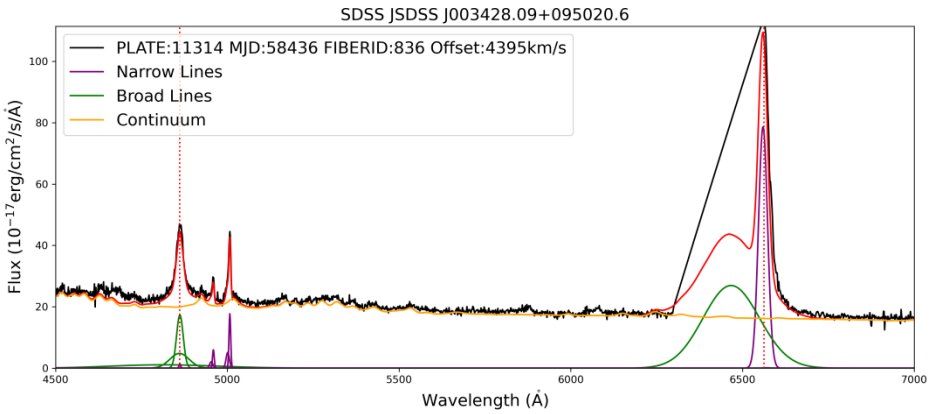

Figure 10: The fitted spectrum of SDSS J003428.09+095020.6, where it is clearly evident that there is a significant loss of data points in the broad emission line region at the red end.

In this study, we identified two samples worthy of further investigation: SDSS J010950.37+335932.9 and SDSS J121522.77+414620.9.

Comparing Figures 3.33 and 3.34, we have the following findings:

There is a significant velocity offset between the broad emission lines and the narrow emission lines, indicating the complexity of gas motion.

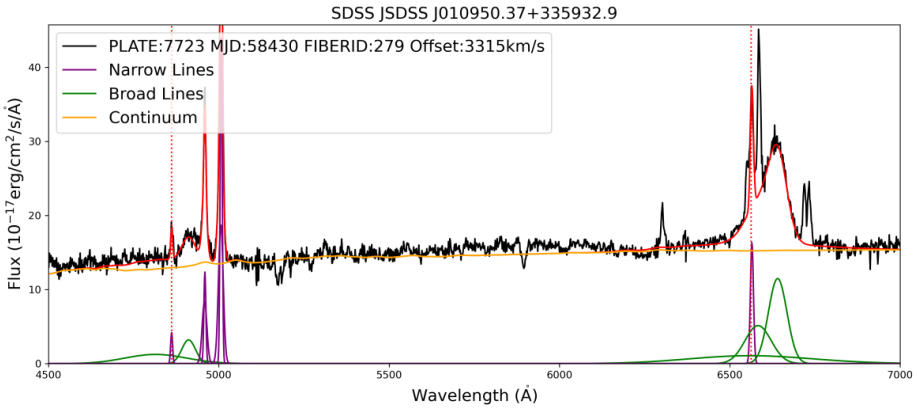

Figure 11: Plate: 7723, MJD: 58430, FiberID: 279, Offset: 3315 km/s. Shows the spectral features of the object, including broad lines (green), narrow lines (purple), and the continuum (yellow). The wavelength range extends from 4500 Å to 7000 Å, with flux in units of (10^-17 erg/cm^2/s/A). At wavelengths of 4862.68 Å and 6564.61 Å, the Hβ and Hα emission lines are marked with red dashed lines.

The broad emission lines on the red side of both spectra are particularly strong, while there are no particularly obvious broad emission lines on the blue side. This characteristic is clearly evident from the broad Hβ and Hα emission lines. The imbalance in the proportion of these broad emission lines is due to dust obscuration. Therefore, the characteristics of the galaxy are highlighted in the spectrum.

DOI: 10.54254/2753-8818/100/2025.21443

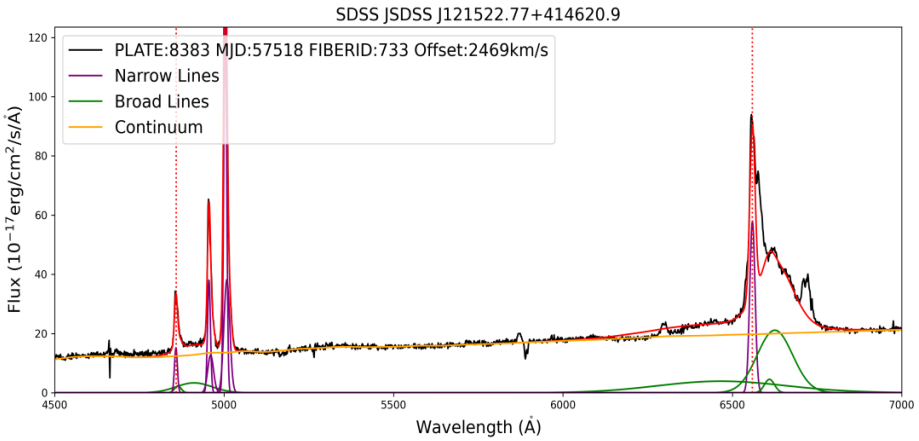

Figure 12: Plate: 8383, MJD: 57518, FiberID: 733, Offset: 2469 km/s. Shows the spectral features of the object, including broad lines (green), narrow lines (purple), and the continuum (yellow). The wavelength range extends from 4500 Å to 7000 Å, with flux in units of (10^-17 erg/cm^2/s/A). At wavelengths of 4862.68 Å and 6564.61 Å, the Hβ and Hα emission lines are marked with red dashed lines

The broad Hβ lines are much weaker than the broad Hα lines, with the intensity ratio and average spectrum being abnormal, whereas their narrow line intensities are higher than normal. This abnormal ratio reveals the extent of dust influence on the emission lines, indicating that dust is primarily distributed in the inner regions of the quasar.

Precisely because the nuclear region of the quasar is obscured by dust, the originally much weaker radiation of the galaxy compared to the quasar becomes observable, manifesting as the presence of obvious galaxy components in the spectrum.

3.4. Host Galaxies with Binary Black Holes

Based on our spectral study, we have determined that the dust is located in the quasar. The central region of the quasar may be obscured by dust, leading to the strong radiation from the quasar core being absorbed or scattered, which makes the originally weaker galaxy components (such as starlight or narrow emission lines) in the quasar spectrum more prominent. This dust obscuration phenomenon is manifested in the spectrum as an abnormal intensity ratio between broad emission lines and narrow emission lines, as well as reddening of the spectrum.

Because the nuclear region of the quasar is partially obscured, the spectral features of other parts of the galaxy become prominent, helping us better understand the characteristics of galaxies hosting binary black holes and further analyze their properties.

4. Results

First, data were extracted from the spectral fitting results of DR16 QSOs and filtered based on redshift and signal-to-noise ratio to ensure that the sample could detect the Hα emission line and maintain a good signal-to-noise ratio. The program retrieved relevant information for SDSS JSDSS J121522.77+414620.9, including the SDSS designation, instrument, plate number, MJD (Modified Julian Date), FiberID, and redshift value.

DOI: 10.54254/2753-8818/100/2025.21443

Row index=8905

SDSS_NAME	PLATE	MJD	FIBERID	RA	DEC	OBJID	IF_BOSS_SDSS	Z_DR16Q	SOURCE_Z_DR16Q	
bytes18	int64	int64	int64	float64	float64	bytes20	bytes10	float64	bytes12	
121522.77+414620.9	8383	57518	733	183.84491323768503	41.77249753323033	8383-57518-0733	BOSS	0.19654589891433716	PIPE	0.1965

Figure 13: The information of SDSS JSDSS J121522.77+414620.9 with image number 8905 read by this program. The output values include the SDSS name, instrument, plate number, MJD (Modified Julian Date), FiberID, and redshift value, among others.

Further fitting parameters for the continuum and Fe[II] pseudo-continuum were extracted, and the Fe[II] templates were loaded. Subsequently, based on the instrument type and plate number, folder paths were set, and the total spectrum files were read, extracting the wavelength and target spectral flux to construct the complete spectral data.

After obtaining the spectral data, we performed dereddening by using SFDQuery to query the dust extinction and employing the F19 parameter average model to calculate the extinction values. The spectral data were then divided by these extinction values. Following this, redshift correction was applied by dividing the wavelength by (1+z) and multiplying the flux by (1+z) to obtain the spectrum in the observer's frame.

By overlaying the continuum model and the Fe[II] pseudo-continuum model, we generated the complete spectral model. We then read the output files of the fitting results to construct the broad and narrow line models for Hα and Hβ, as well as the [OIII] doublet and other narrow line models. By adjusting the plotting range and plotting the observed spectrum alongside the model spectrum, the fit between the model and the observational data can be visually assessed.

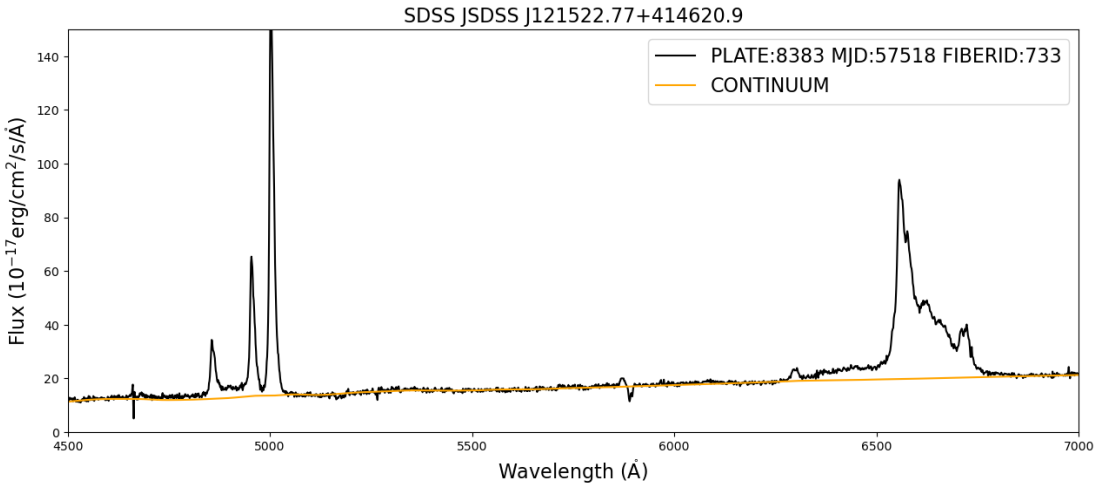

Figure 14: Spectrum after overlaying the continuum emission lines.

DOI: 10.54254/2753-8818/100/2025.21443

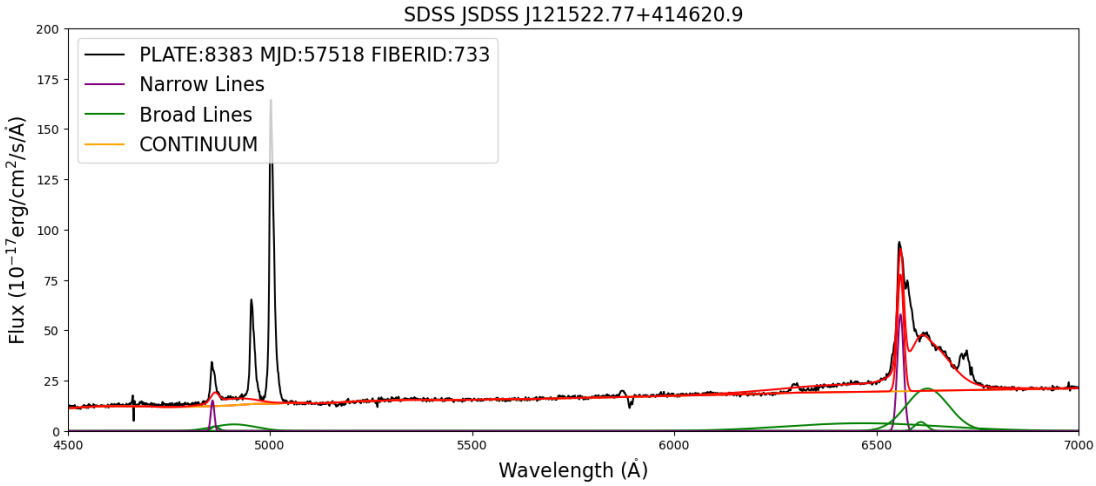

Figure 15: Spectrum after overlaying the broad Hα and Hβ emission lines.

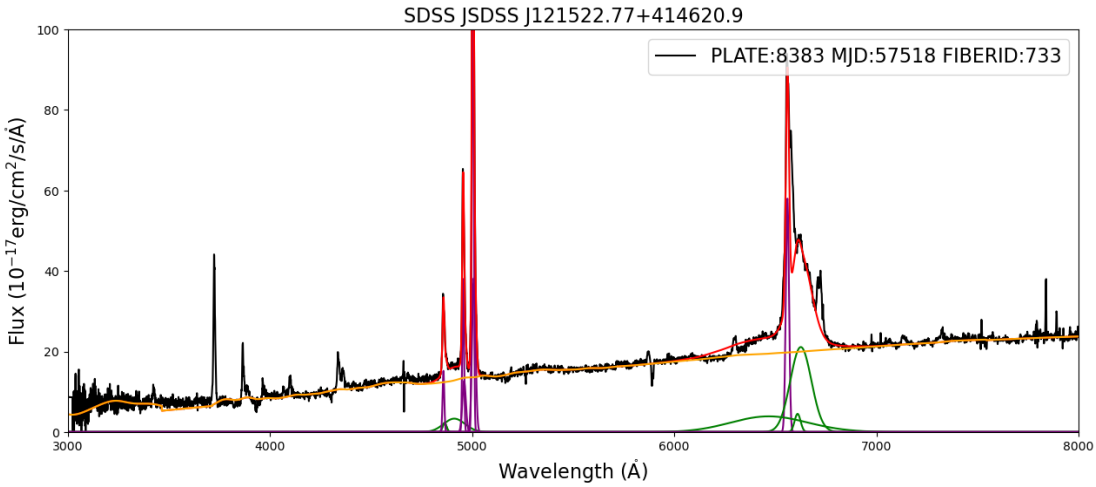

Figure 16: Spectrum after overlaying the narrow [O III] emission lines.

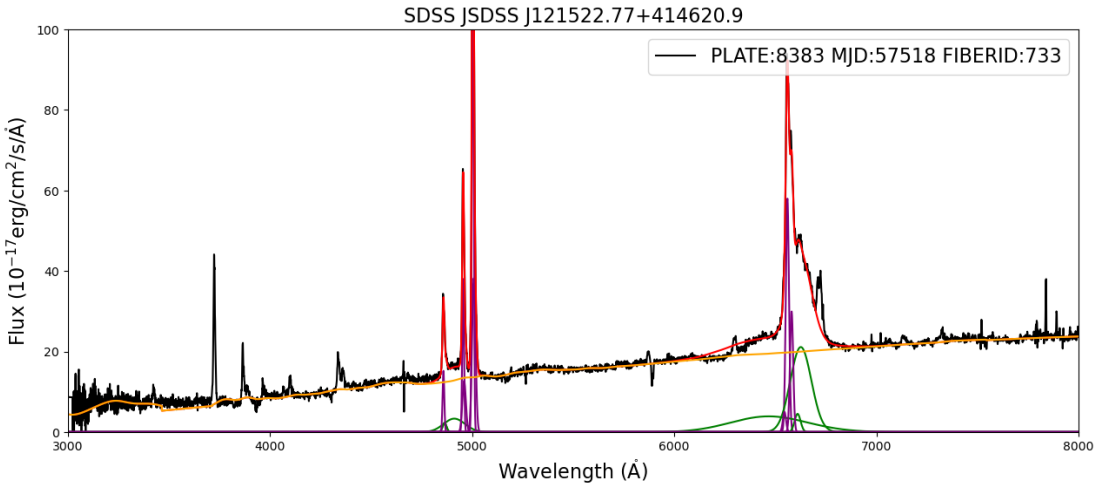

Figure 17: Spectrum after overlaying the narrow [N II] emission lines.

DOI: 10.54254/2753-8818/100/2025.21443

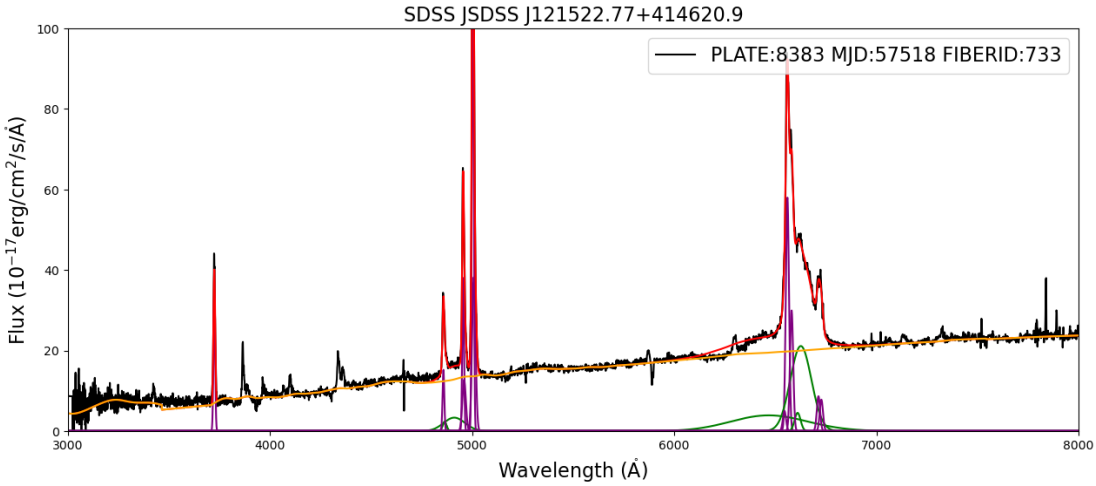

Figure 18: Spectrum after overlaying additional narrow emission lines.

Finally, we obtained the galaxy's spectrum by subtracting the quasar's spectrum from the observed spectrum.

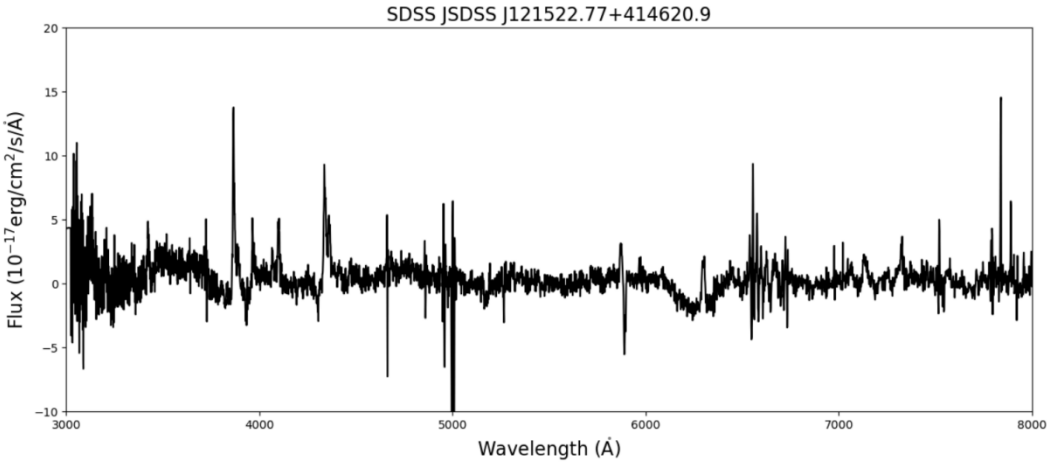

Figure 19: The host galactic spectrum of SDSS J121522.77+414620.9

Then, the program calculates the black hole mass using the FWHM (Full Width at Half Maximum) of the Hα line and the luminosity at 5100 Å, through the following formula for black hole mass

$$log\left(\frac{M_{BH}}{M_{\odot}}\right) = 0.91 + 0.50\, log\left(\frac{5100L_{5100}}{10^{44} erg\ s^{-1}}\right) + 2\, log\left(\frac{FWHM}{km\ s^{-1}}\right) \quad (4)$$

This formula combines the width of the Hα line and the luminosity of the quasar to ultimately estimate the black hole mass, with units in solar masses. L_{5100} is the luminosity of the quasar at 5100 Å, and FWHM is the Full Width at Half Maximum of the Hα line.

In this example, the calculations yield: $L_{5100} = 7.5 \times 10^{43}\ erg$ and FWHM = 5383 km/s. Substituting these values into the formula, the black hole mass of SDSS J121522.77+414620.9 is estimated to be approximately 1.46×10^{10} solar masses. This calculation result is based on a detailed analysis of the observational data and model fitting, providing us with important information about the characteristics of the target black hole.

DOI: 10.54254/2753-8818/100/2025.21443

```
In [52]: FWHM = qsos['HALPHA_BR'][num][4]
         L5100 = 10**qsos['LOGL5100'][num]

In [53]: L5100 # QSO's Luminosity at rest frame wavelength 5100

Out[53]: 7.490453327638154e+43

In [54]: FWHM # width of Halpha

Out[54]: 5382.930466206552

In [55]: mass = 0.91 + 0.5*np.log10(5100*L5100*10.0**(-44)) + 2*np.log10(FWHM)

In [56]: mass = 10**mass

In [57]: mass # in unit of Solar mass

Out[57]: 14557160788.235401
```

Figure 20: Calculation of black hole mass for SDSS J121522.77+414620.9

Similarly, we also plotted the spectra of SDSS J010950.37+335932.9 and calculated its black hole mass to be 6.69×10^9 solar masses.

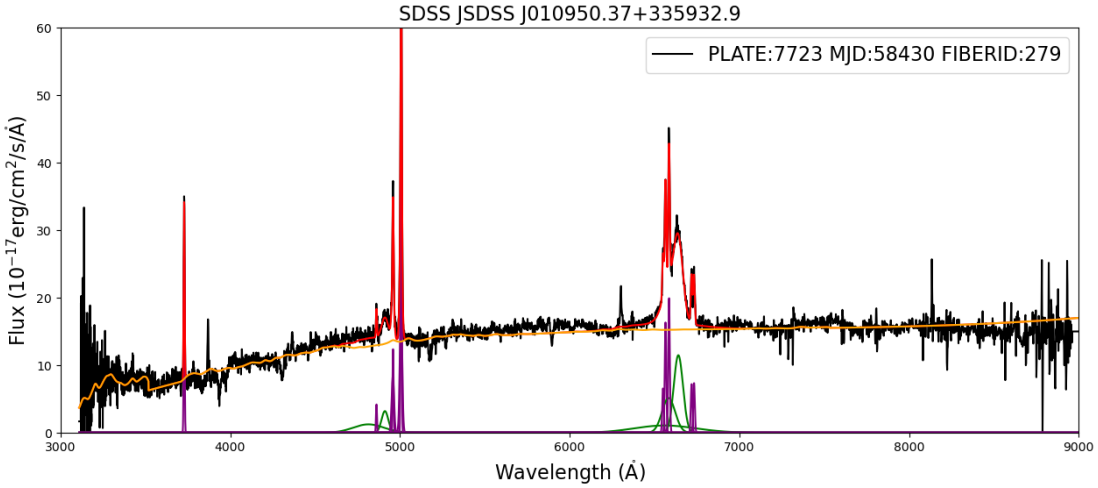

Figure 21: Spectrum of SDSS J010950.37+335932.9

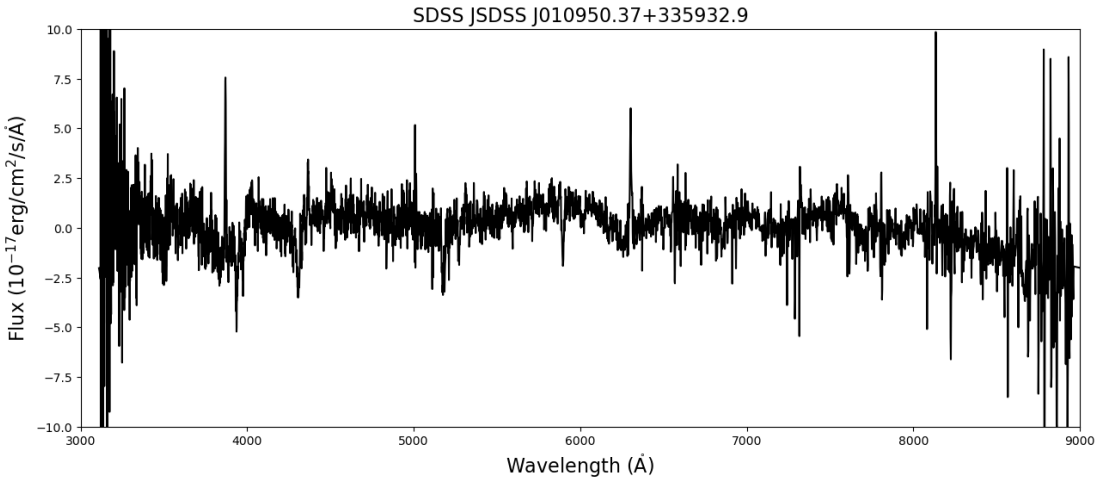

Figure 22: Spectrum of the host galaxy of SDSS J010950.37+335932.9

DOI: 10.54254/2753-8818/100/2025.21443

5. Conclusion

In this study, we delved deeply into the dynamic evolution of SMBHs during galaxy mergers and their profound impact on host galaxies. Through detailed spectral analyses of the galaxies SDSS J121522.77+414620.9 and SDSS J010950.37+335932.9, we revealed their unique positions in the universe and, based on this, reviewed previous research on galaxy mergers, the formation of binary black holes, and the consequent triggered star formation.

Firstly, the galaxies SDSS J121522.77+414620.9 and SDSS J010950.37+335932.9 stand out due to their prominent binary black hole features. By meticulously analyzing the spectral data of these galaxies, we discovered significant velocity offsets between the broad and narrow emission lines, strongly suggesting the presence of binary black hole systems. These velocity offsets not only provide direct evidence of the gravitational interactions between binary black holes but also offer valuable information for studying the black hole merger process.

From a broader academic perspective, our research engages in dialogue with previous studies in the field of binary black hole formation through galaxy mergers. Studies have shown that galaxy mergers are a crucial pathway for the growth of SMBHs in the universe. During mergers, the SMBHs at the centers of the two galaxies rapidly sink toward a common gravitational center through dynamical friction, ultimately forming a binary black hole system. This process involves not only complex gravitational dynamics but is also closely related to the gas dynamics within the galaxies. The inflow of gas provides fuel for the black holes, promoting their growth SMBHs and simultaneously triggering star formation.

Additionally, our research touches upon the impact of binary black hole systems on the evolution of their host galaxies. During the interactions and eventual mergers of binary black holes, the intense gravitational wave radiation can impart recoil velocities to the black holes, thereby affecting the dynamical structure of the galaxy's center. Although the phenomenon of "black hole recoil" has been widely discussed theoretically, it remains rare in actual observations. The study of SDSS J092712.65+294344.0 provides a potential case of a recoiling black hole, offering valuable clues for understanding this phenomenon.

In terms of triggering star formation, our research emphasizes the connection between binary black hole systems and star formation within galactic nuclei. The gravitational interactions in binary black hole systems can induce the collapse of gas in the galaxy's center, thereby initiating new rounds of star formation. This process is significant for comprehending galaxy evolution and the history of star formation in the universe.

Although, at present, due to low signal-to-noise ratios in the data, we have been unable to analyze the specific parameters of the host galaxies, we have, for the first time, identified a class of targets that allow for the simultaneous study of binary black holes and their host galaxies. We believe that using large-aperture telescopes (such as the 10-meter Keck Telescope) for spectral observations will undoubtedly yield more detailed results. Conversely, if the AGN is partially obscured by dust, it would be impossible to discern the galaxy's components even with the largest telescopes. Therefore, the significance of our work lies in identifying an important class of targets that can be used to study host galaxies with binary black holes, thereby enhancing our understanding of the coevolution of black holes and galaxies. The unique status of the galaxies SDSS J121522.77+414620.9 and SDSS J010950.37+335932.9 not only highlights them as candidates for binary black hole systems but also provides us with clues for studying galaxy mergers, black hole mergers, and the resultant star formation. Our research not only advances the understanding of these complex astronomical phenomena but also offers new directions for future observational and theoretical studies.

DOI: 10.54254/2753-8818/100/2025.21443

References

[1] *Ferrarese, Laura, and David Merritt. "A Fundamental Relation Between Supermassive Black Holes and Their Host Galaxies." The Astrophysical Journal, vol. 539, 2000, pp. L9-L12. DOI: 10.1086/317296.*

[2] *Eracleous, Michael, et al. "A LARGE SYSTEMATIC SEARCH FOR CLOSE SUPERMASSIVE BINARY AND RAPIDLY RECOILING BLACK HOLES." The Astrophysical Journal Supplement Series, vol. 201, 2012, pp. 23. JSTOR, doi:10.1088/0067-0049/201/2/23.*

[3] *Ferrarese, Laura, and David Merritt. "A Fundamental Relation Between Supermassive Black Holes and Their Host Galaxies." The Astrophysical Journal, vol. 539, 2000, pp. L9-L12. DOI: 10.1086/317296.*

[4] *Maoz, Dan. Astrophysics in a Nutshell. Princeton Princeton University Press, 2016.*

[5] *Peterson, Bradley M. An Introduction to Active Galactic Nuclei. Cambridge, University Press, 1997.*

[6] *Komossa, S., et al. "A RECOILING SUPERMASSIVE BLACK HOLE IN THE QUASAR SDSS J092712.65+294344.0?" The Astrophysical Journal, vol. 678, 2008, pp. L81–L84. JSTOR, doi:10.1086/588585.*

[7] *Wilkinson, David M., et al. "FIREFLY (Fitting IteRativEly For Likelihood analYsis): a full spectral fitting code." Monthly Notices of the Royal Astronomical Society, vol. 472, no. 4, 2017, pp. 4297–4326. DOI: 10.1093/mnras/stx2215.*

[8] *Wu, Qiaoya, and Yue Shen. "A Catalog of Quasar Properties from Sloan Digital Sky Survey Data Release 16." The Astrophysical Journal Supplement Series, vol. 263, no. 42, 2022, pp. 1-12. DOI: 10.3847/1538-4365/ac9ead.*

Appendix: Spectra of 20 more Binary Black Hole Candidates

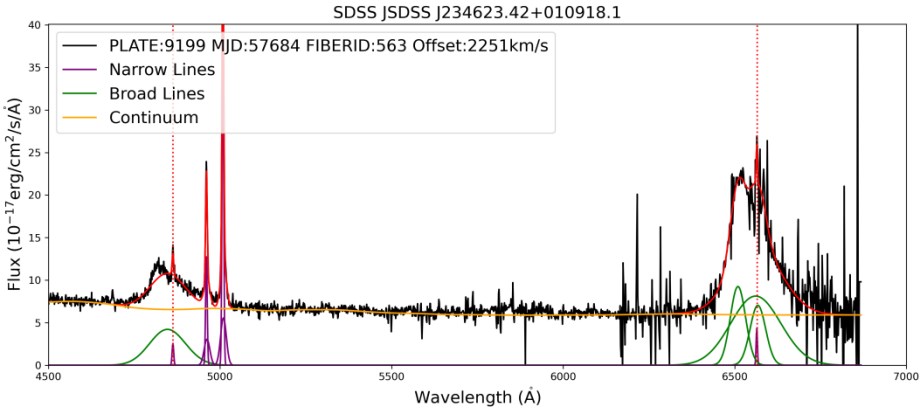

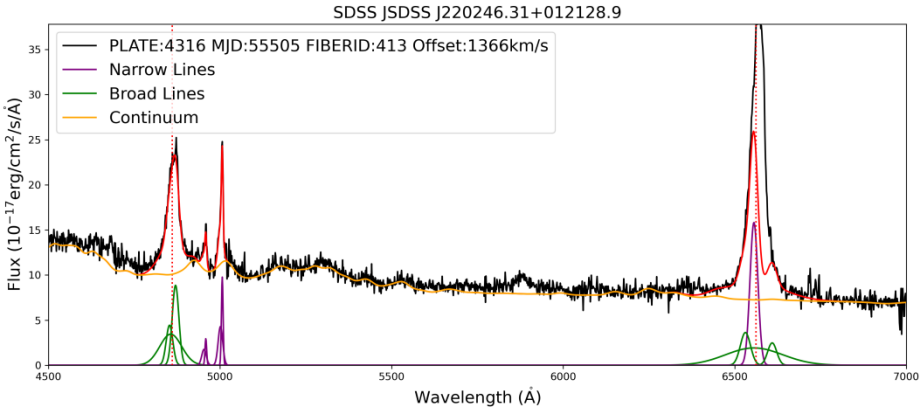

DOI: 10.54254/2753-8818/100/2025.21443

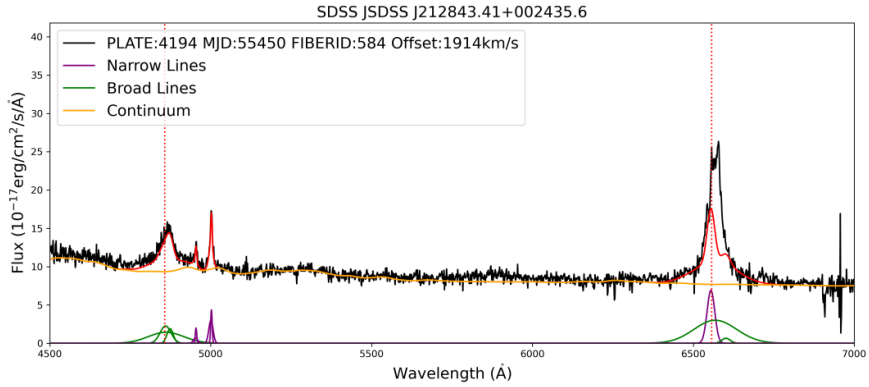

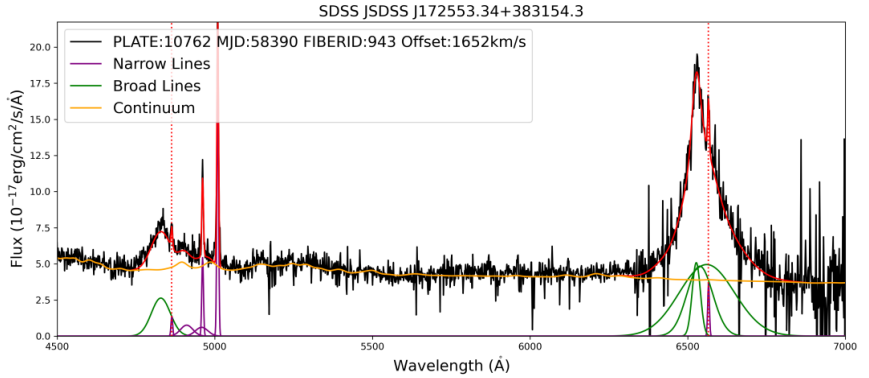

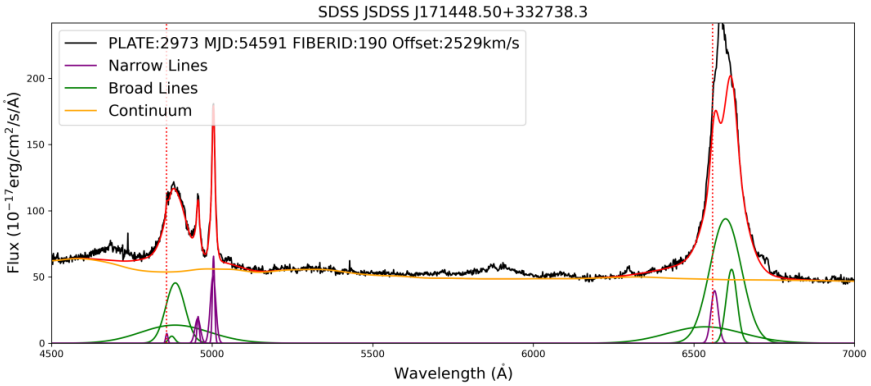

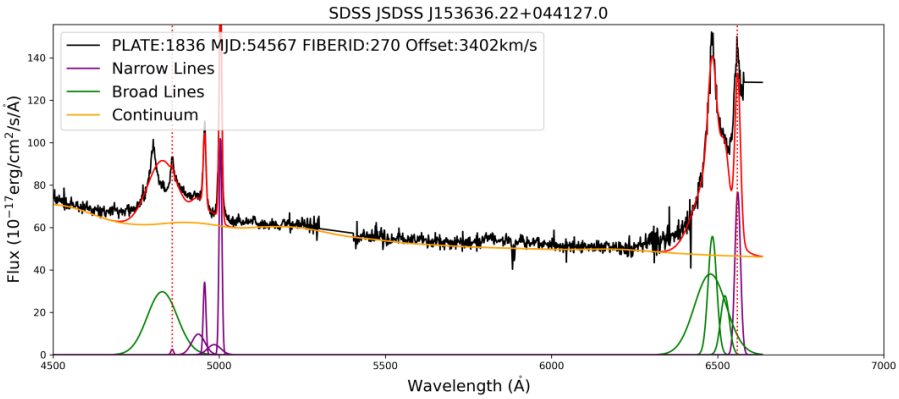

DOI: 10.54254/2753-8818/100/2025.21443

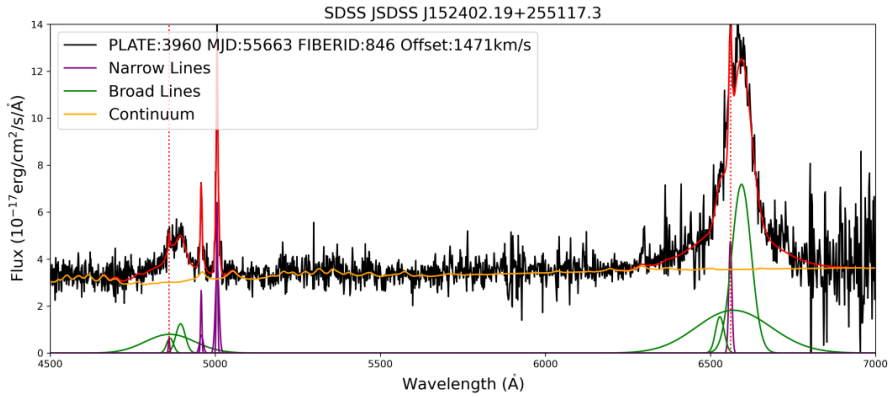

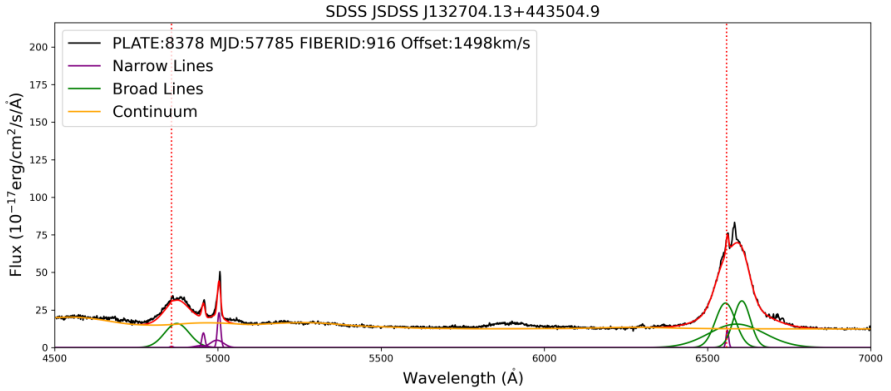

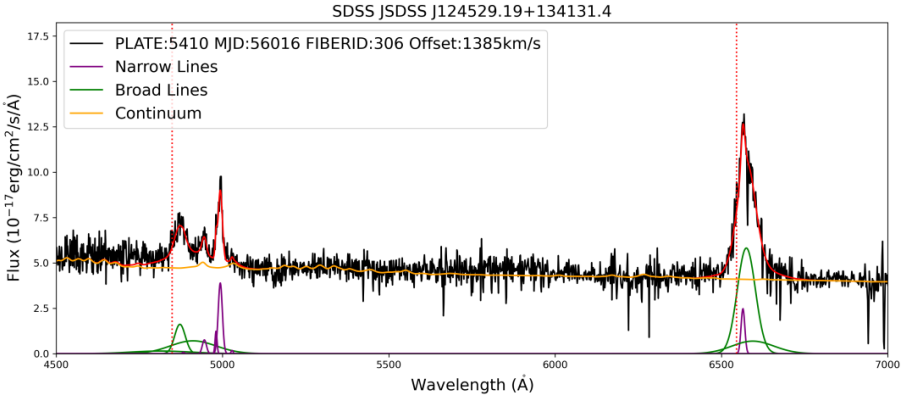

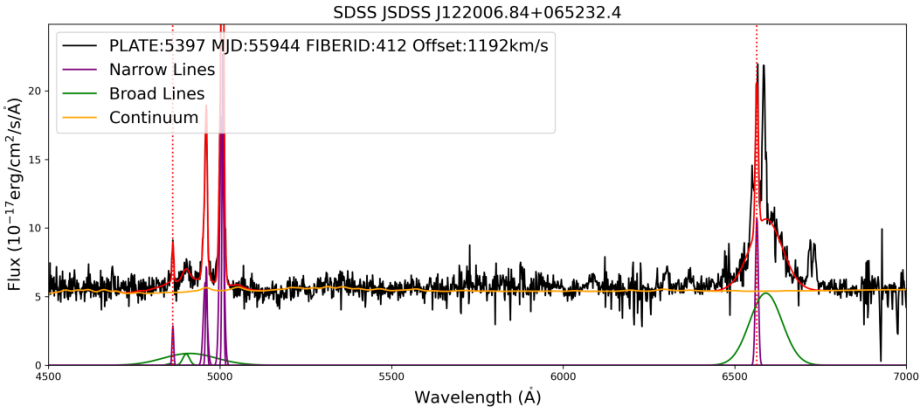

DOI: 10.54254/2753-8818/100/2025.21443

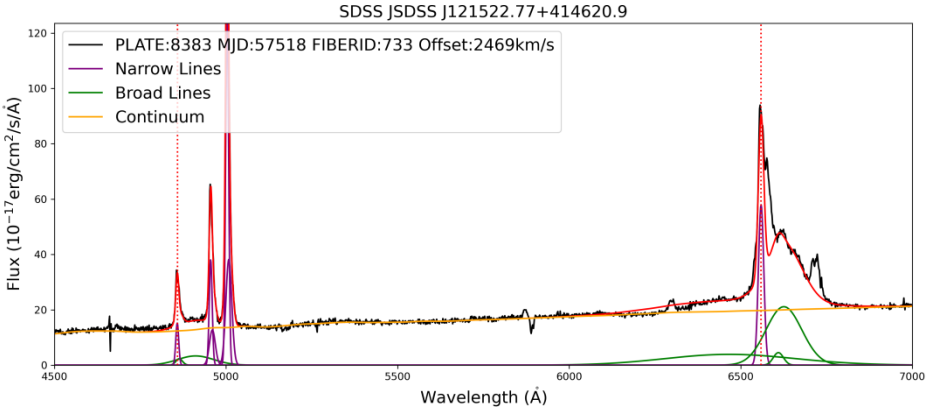

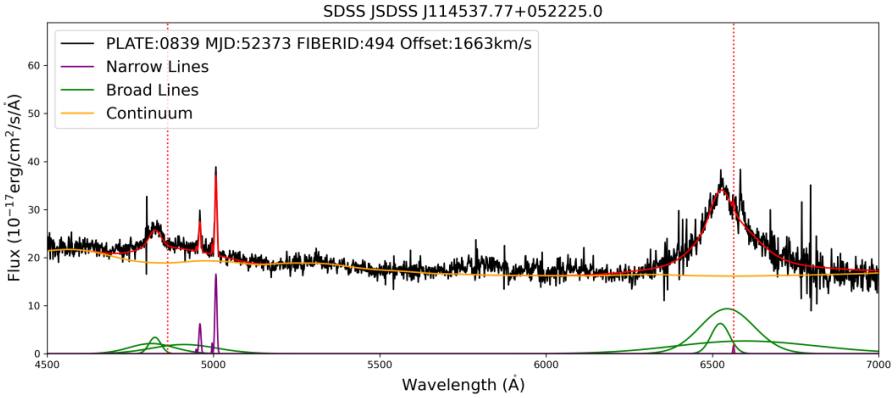

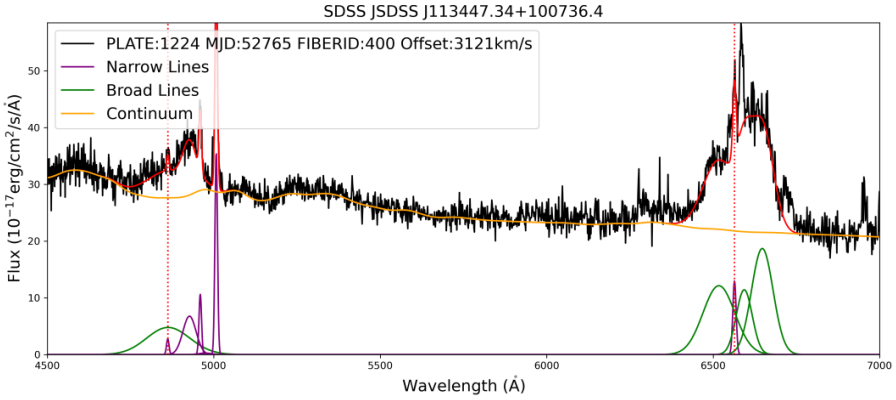

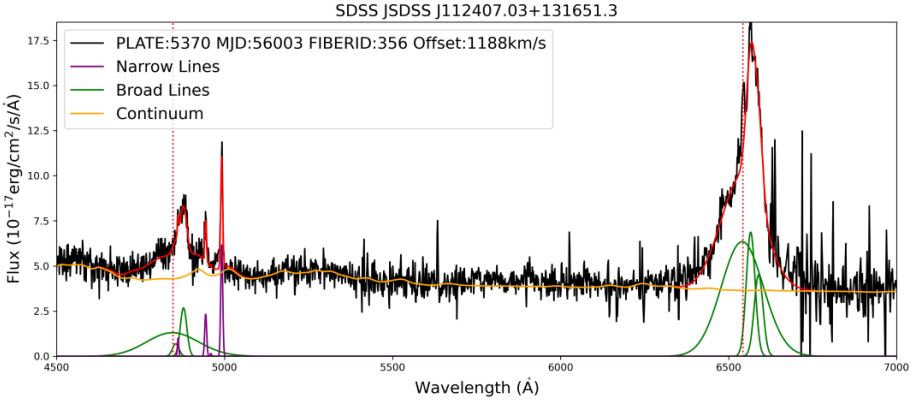

DOI: 10.54254/2753-8818/100/2025.21443

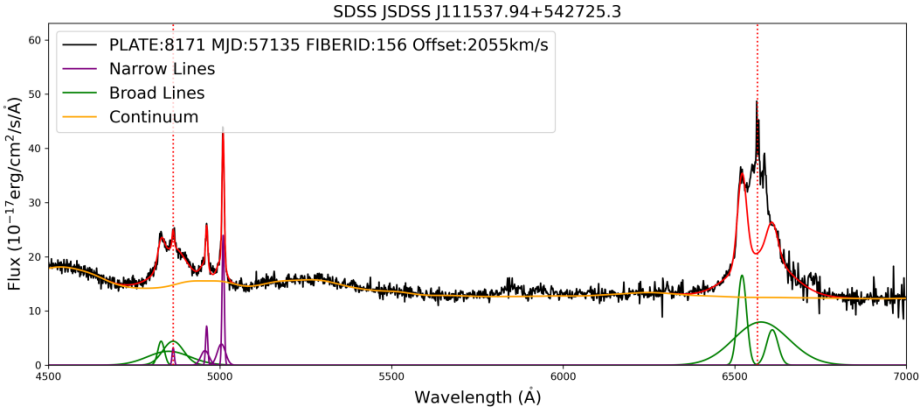

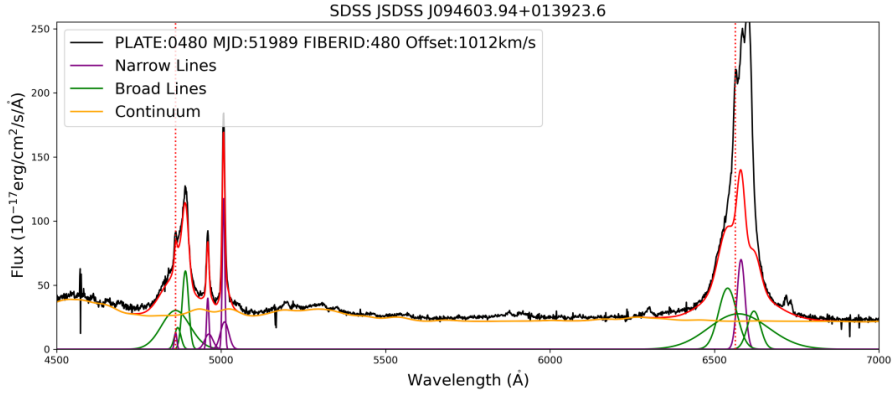

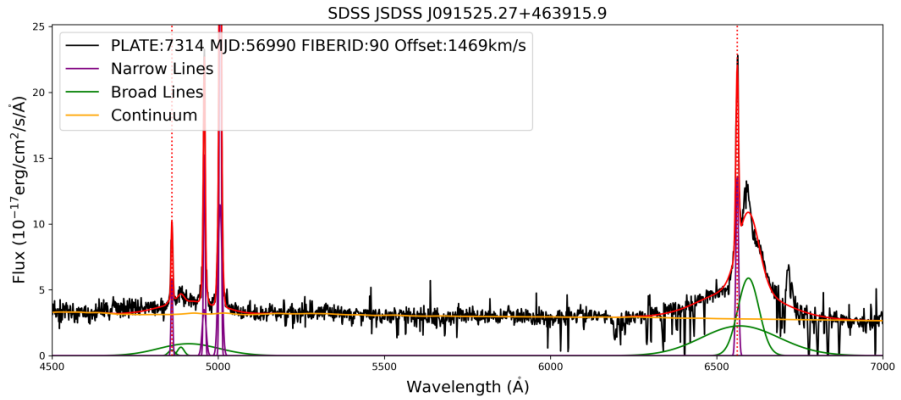

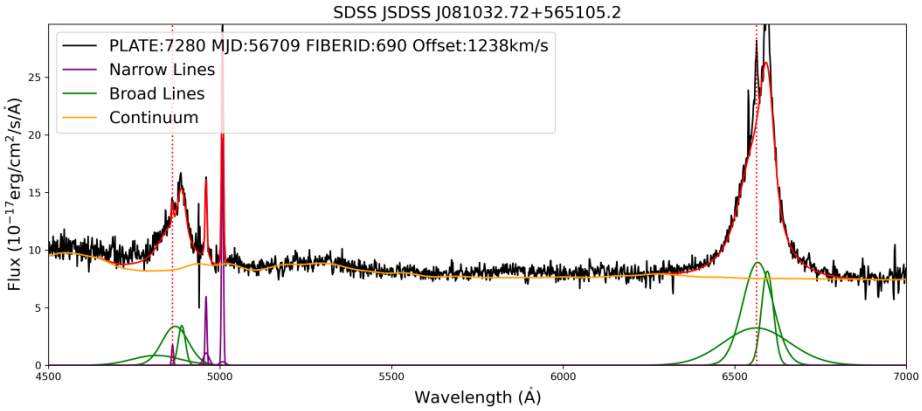

DOI: 10.54254/2753-8818/100/2025.21443